

SI material for:

Assessment of the manganese cluster's oxidation state *via* photoactivation of photosystem II microcrystals

Mun Hon Cheah<sup>a,1,2</sup>, Miao Zhang<sup>b,1</sup>, Dmitry Shevela<sup>c</sup>, Fikret Mamedov<sup>a</sup>, Athina Zouni<sup>b,2</sup>, Johannes Messinger<sup>a,c,2</sup>

<sup>a</sup> Molecular Biomimetics, Department of Chemistry – Ångström Laboratory, Uppsala University, 75120 Uppsala, Sweden

<sup>b</sup> Institut für Biologie, Humboldt-Universität zu Berlin, 10115, Berlin, Germany

<sup>c</sup> Department of Chemistry, Chemical Biological Centre, Umeå University, 90187, Umeå, Sweden

<sup>1</sup> contributed equally

<sup>2</sup> Corresponding authors:

Mun Hon Cheah, Molecular Biomimetics, Department of Chemistry – Ångström Laboratory, Uppsala University, Box 523, SE-75120 Uppsala, Sweden; phone: +46(73)8030682, email: [michael.cheah@kemi.uu.se](mailto:michael.cheah@kemi.uu.se)

Athina Zouni, Institut für Biologie, Humboldt-Universität zu Berlin, Philippstraße 13, D-10115 Berlin, Germany, phone: +49(0)30209347930, email: [athina.zouni@hu-berlin.de](mailto:athina.zouni@hu-berlin.de)

Johannes Messinger, Molecular Biomimetics, Department of Chemistry – Ångström Laboratory, Uppsala University, Box 523, SE-75120 Uppsala, Sweden; phone: +46(70)1679843, email: [johannes.messinger@kemi.uu.se](mailto:johannes.messinger@kemi.uu.se)

This PDF file includes:

Supplementary text

Figures S1 to S4

SI references

## SI text

### Estimation of residual NH<sub>2</sub>OH concentration

The NH<sub>2</sub>OH and EDTA employed during the manganese depletion procedure were removed from apo-PSII microcrystals with eight washing and two dialysis steps. The dilution factor of each washing step was between 0.3 to 0.5 and the dilution factor of each dialysis step was 0.024. We estimate the residual NH<sub>2</sub>OH and EDTA concentration to be in the range between  $50 \text{ mM} \times (0.3)^8 \times (0.024)^2 = 0.2 \text{ nM}$  to  $0.1 \text{ }\mu\text{M}$ .

### Estimation of average quantum yield of photoactivation

The average quantum yield of photoactivation was estimated based on the observation that the O<sub>2</sub> yield after the 9<sup>th</sup> flash during photoactivation was approximately 0.1% of that obtained from native PSII after the 3<sup>rd</sup> flash. It is reasonable to assume the quantum yield from S<sub>1</sub> to higher S states are equivalent for photoactivated-PSII and for native PSII, therefore the overall quantum yield of photoactivation of apo-PSII for the first six flashes, i.e. from 4 times Mn<sup>2+</sup> up to the S<sub>1</sub> state, is also 0.1%. The average quantum yield is then estimated as  $(0.001)^{1/6} = 0.32$  or 32%. While typical reported quantum yields are 1% (1-3), Miyao-Tokutomi and Inoue reported a quantum yield of 19% (4) that is comparable to our results.

It should be noted that reports stating quantum yields for photoactivation of 1% were calculated based on estimated recovery of PSII activity that is measured as gross rate of oxygen evolution under continuous illumination. On the other hand, the quantum yield of our experiment was calculated directly from the amount of O<sub>2</sub> evolved during photoactivation, i.e. are a direct measure of photoactivated PSII.

### Peak fitting of oxygen signals

The oxygen yields of the FIOP are estimated from m/z 34 oxygen signals using the multipeak fitting procedure implemented in Igor Pro 6.3 (WaveMetrics) and described below.

Each flash induced oxygen peak was fitting to a peak profile that is a convolution of two exponentials of the general form:

$$(\exp(-k_1*t) - \exp(-k_2*t))*k_1*k_2/(k_2-k_1)$$

Where  $k_1$  describes the rise and  $k_2$  describes the fall of the peak;  $k_1 > k_2$ . The whole FIOP trace was fitted as the sum of individual oxygen peaks that were spaced 15 seconds apart, each peak sharing the same  $k_1$  and  $k_2$  parameters. The oxygen yield was calculated from the area under each fitted peak. Confidence interval of the oxygen yield at 95% level ( $2\sigma$ ) was calculated from standard deviations of the peak amplitude derived from the fitting procedure.

The Igor Pro 6.3 script is presented below.

```
Function fExpConvExpFit2Shape(w,x)
    Wave w; Variable x

    Variable r= w[0]
    Variable expRise= w[1], expDecay= w[2], Peak0pos=w[3], Peak2Peak=w[4]
        //expRise is k1, expDecay is k2, Peak0pos is peak position of first peak
        // Peak2Peak is separation between peaks
    variable npts= numpnts(w),i=4
    do
    if( i>=npts )
        break
    endif
        r += (w[i]/expRise)*fExpConvExp(x-(Peak0pos+(i-5)*Peak2Peak),expRise,
            expDecay) // w[i] is amplitude
    i+=1
    while(1)
    return r
End
```

### **Estimation of oxygen detection limit**

The oxygen detection limit was estimated by the following procedure. A single peak function with defined peak area was generated using the equation presented above for the peak fitting procedure (Figure S1 blue dashed line). Random noise at a level comparable to experimental data was added to the peak function to obtain a simulated signal (Figure S1 red line). The peak area of the simulated signal was then estimated using the peak fitting procedure presented above (Figure S1 black line). This procedure was repeated multiple times with various defined peak areas (Figure S2). We chose to define the detection limit when 95% ( $2\sigma$ ) of the fitted peak area is above zero, which corresponds to value of 0.024 arbitrary units. Based on the oxygen yield

obtained from single turnover of pristine PSII (after 3 flashes), this corresponded to an oxygen concentration of approximately 3 nM.

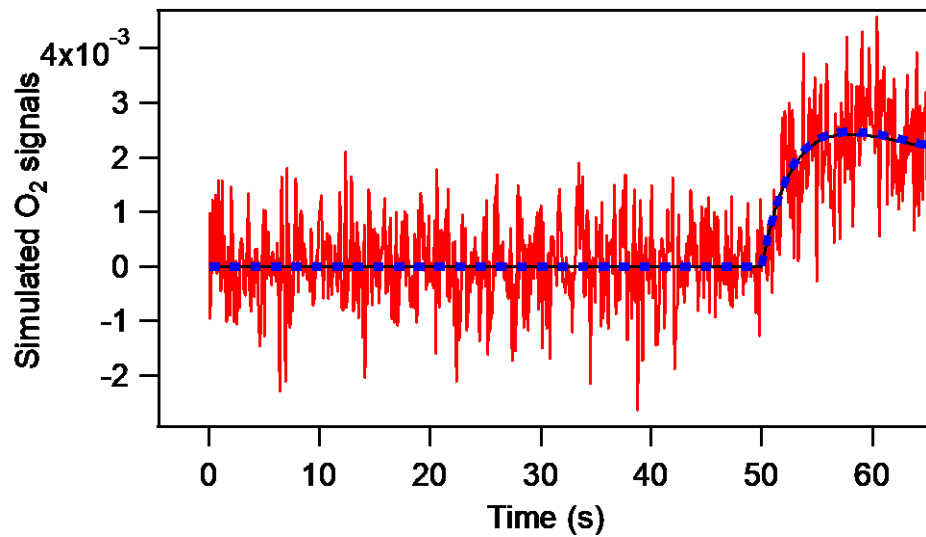


**Figure S1.** Peak function with pre-defined area (blue dash line). Simulated signal (Red line). Result of peak fitting of simulated signal (black line).

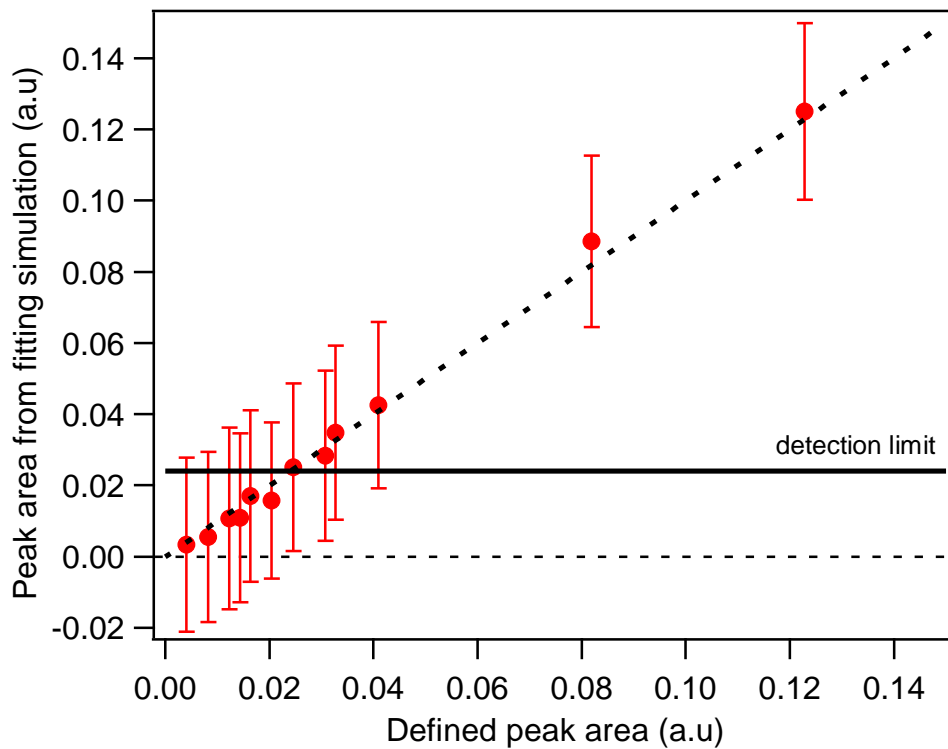


**Figure S2.** Estimated peak area from fitting simulated signals as a function of pre-defined peak areas. Error bars are 95% confidence interval ( $2\sigma$ ) derived from standard deviations of fitted peak amplitude.

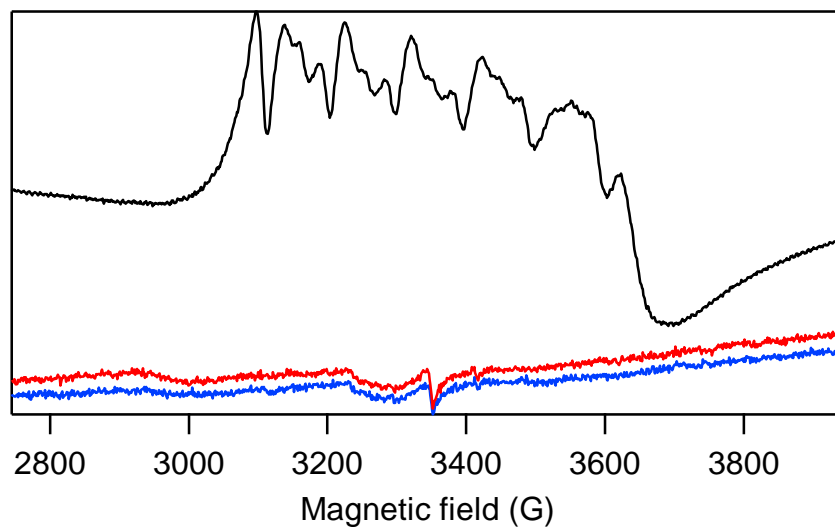


**Figure S3:** Estimation of the Mn content in the apo-PSII microcrystals by EPR measurements. The spectra shown are of 10  $\mu\text{M}$   $\text{MnCl}_2$  in MIMS buffer (0.1 M MES pH 6.5, 0.1 M  $\text{NH}_4\text{Cl}$ , 20% PEG 5000) (black line), of 0.5 mM apo-PSII microcrystals in MIMS buffer (blue line) and of 0.5 mM apo-PSII microcrystals in MIMS buffer after heat treatment at 363 K for 10 minutes (red line). Both EPR spectra of apo-PSII microcrystals were magnified by 10-times. All spectra were offset from zero for clarity. The EPR measurements were done with Bruker ELEXSYS E500 spectrometer (Bruker BioSpin) using a SuperX EPR049 microwave bridge and SHQ4122 cavity. The system was fitted with a liquid helium 900 cryostat and ITC503 temperature controller from Oxford Instruments Ltd. EPR conditions: Microwave frequency 9.38 GHz, microwave power 10 mW, modulation amplitude 15 G, temperature 15 K.

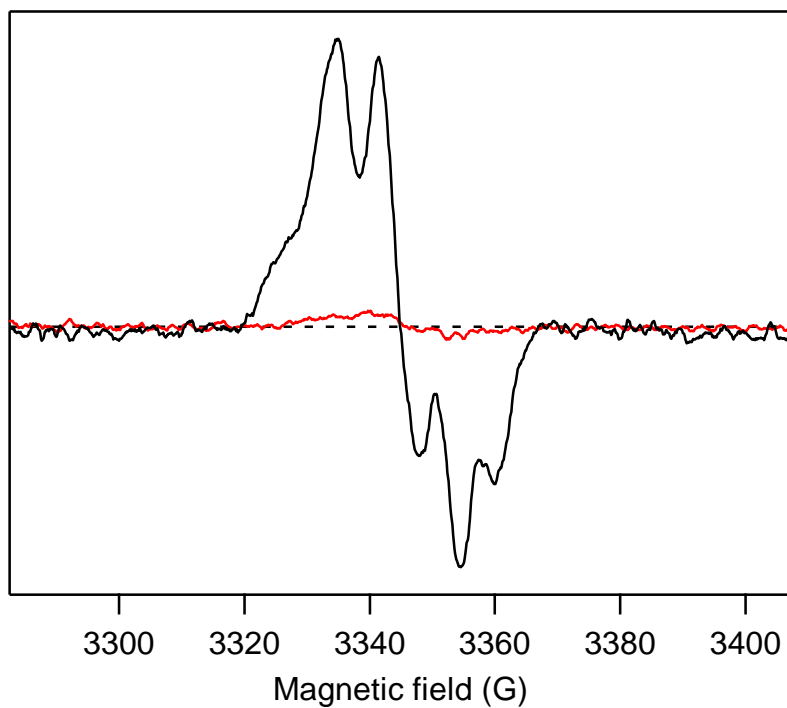


**Figure S4:** Measurements of Tyrosine D radical in the apo-PSII microcrystals by EPR spectroscopy. The spectra shown are of apo-PSII microcrystals in the dark (red line) and of the maximum inducible Tyrosine D radical by room light illumination for 2 min at room temperature. EPR conditions were as in Figure S3, except that a microwave power of 1.3  $\mu$ W and a modulation amplitude of 3.5 G were employed.



## References

1. G. M. Cheniae, I. F. Martin, Photoactivation of the manganese catalyst of O<sub>2</sub> evolution. I. Biochemical and kinetic aspects. *Biochimica et Biophysica Acta (BBA) - Bioenergetics* **253**, 167-181 (1971).
2. R. Radmer, G. M. Cheniae, Photoactivation of the manganese catalyst of O<sub>2</sub> evolution. II. A two-quantum mechanism. *Biochimica et Biophysica Acta (BBA) - Bioenergetics* **253**, 182-186 (1971).
3. N. Tamura, G. Cheniae, Photoactivation of the water-oxidizing complex in Photosystem II membranes depleted of Mn and extrinsic proteins. I. Biochemical and kinetic characterization. *Biochimica et Biophysica Acta (BBA) - Bioenergetics* **890**, 179-194 (1987).
4. M. Miyao-Tokutomi, Y. Inoue, Improvement by benzoquinones of the quantum yield of photoactivation of photosynthetic oxygen evolution: direct evidence for the two-quantum mechanism. *Biochemistry* **31**, 526-532 (1992).